Biochimica et Biophysica Acta, 984 (1989) 128–134
Elsevier

BBAMEM 74535

Restricted lateral diffusion of acidic lipids in phospholipid vesicles aggregated by myelin basic protein

T. Páli and L.I. Horváth

Institute of Biophysics, Biological Research Center, Szeged (Hungary)

(Received 17 February 1989)
(Revised manuscript received 29 May 1989)

Key words: Lipid lateral diffusion; Lipid–protein interaction; Myelin basic protein; Spin label; ESR

The effect of myelin basic protein on the lateral diffusion of spin-labelled stearic acid in dimyristoylphosphatidylcholine (DMPC) and dimyristoylphosphatidylglycerol (DMPG) vesicles has been investigated measuring bimolecular collision rates by electron spin resonance spectroscopy. In a molar fraction range of 0.02–0.15, in which the line shape is dominated by the effects of exchange narrowing and dipolar broadening, spectral simulations based on the modified Bloch equations have been used to quantitate the observed spectral changes. Best fitting simulated spectra required a combination of dipole-dipole and spin exchange contributions and least-squares optimizations were applied to obtain a unique combination of these factors. Lateral diffusion coefficients were calculated from collision frequency data in the frame of the lattice model; for pure DMPC and DMPG vesicles lateral diffusion coefficients of $1.7 \cdot 10^{-7}$ and $1.2 \cdot 10^{-7}$ cm$^2 \cdot$ s^{-1} were obtained. Upon adding myelin basic protein to these vesicles the diffusion coefficients of the negatively charged DMPG decreased to $4.1 \cdot 10^{-8}$ cm$^2 \cdot$ s^{-1}, whereas that of the zwitterionic DMPC remained unchanged. It is concluded that myelin basic protein must strongly restrict the lateral movement of the DMPG molecules and reduce their diffusion coefficient close to the values observed for proteins. The restricted lateral diffusion is explained by electrostatic interactions which lead to an altered molecular dynamics due to one-to-one lipid exchange and lipid-protein co-diffusion.

Introduction

Spin label electron spin resonance (ESR) spectroscopy has optimal sensitivity for studying lipid dynamics in model and biological membranes [1]. Phospholipids and their spin labelled analogues undergo rapid acyl chain isomerization and lateral diffusion in fluid bilayers and so their motionally averaged ESR spectra can readily be resolved from the powder pattern of solvation lipids which are motionally restricted at the interface of integral membrane proteins (for recent reviews see Refs. 2 and 3). The spectral resolution between these two line shapes provides a very powerful means to study the stoichiometry and specificity of lipid–protein interaction [4]. Peripheral membrane proteins, however, are more difficult to investigate by such spectral analyses because the short intramembraneous loops, which are believed to play a central role in anchoring these proteins at membrane interfaces, result in less effective acyl chain immobilization, particularly close to the methyl terminals [5]. In spite of the successful application of spin label ESR to many integral membrane proteins only a few peripheral proteins have been investigated so far; the first results were published on apocytochrome *c* [6,7], glycerol-3-phosphate dehydrogenase [8], lactalbumin [9], and myelin basic protein [5,10,11].

The myelin basic protein (MBP) is a prototype of peripheral proteins and is known to interact preferentially with acidic lipids to neutralize its unmasked basic residues at a stoichiometry of 25–30 mol/mol [11]. Its secondary structure in aqueous solution is devoid of α-helical and β-conformations, but contains a significant amount of turns (16%), while it is dominated by β-sheets (53%) and equal amounts of α-helical and turns (15%) when bound to DMPG bilayers [12]. Basic protein aggregates vesicles of acidic lipids; this effect

Abbreviations: DMPC, dimyristoylphosphatidylcholine; DMPG, dimyristoylphosphatidylglycerol; EDTA, ethylenediaminetetraacetic acid; ESR, electron spin resonance; Hepes, 4-(2-hydroxyethyl)-1-piperazineethanesulfonic acid; MBP, myelin basic protein; 16-SASL, 16-(4′,4′-dimethyloxazolidine-*N*-oxyl)stearic acid.

Correspondence: L.I. Horváth, Institute of Biophysics, Biological Research Center, H-6701 Szeged, P.O. Box 521, Hungary.

was studied by turbidity changes [13] and ESR imaging in conjunction with sedimentation equilibrium experiments [14]. Here we apply lipid lateral diffusion measurements for studying the interaction between basic protein and membrane lipids and demonstrate that there is a restricted lateral diffusion of acidic lipids in the presence of basic protein. It is suggested that certain lipids which selectively interact with basic protein undergo slow co-diffusion with the protein. The role of one-to-one lipid exchange and lipid-protein co-diffusion is discussed as the two major contributions to the altered interfacial dynamics.

Materials and Methods

Materials. 1,2-Dimyristoyl-*sn*-glycerol-3-phosphocholine (DMPC) was obtained from Fluka (Buchs, Switzerland); 1,2-dimyristoyl-*sn*-glycerol-3-phosphoglycerol (DMPG) was provided by Dr. D. Marsh (Göttingen, F.R.G.). Both lipids gave single spots by thin-layer chromatography (solvent system: C_6H_{14}/CH_3OH/33% NH_3 (65 : 30 : 3, v/v) and molybdenum staining followed by sulfuric acid charring) and were used without further purification. C-16 positional isomer of spin-labelled stearic acid (16-SASL) was obtained from Aldrich Chemical Co. (Beerse, Belgium). Myelin basic protein was purified by Dr. G.J. Tigyi of this Institute as described in Ref. 15.

Preparation of lipid vesicles. Lipid and spin probe at different ratios were mixed in chloroform/methanol, evaporated to dryness by N_2 gas stream, and evacuated for several hours to remove solvent traces. Lipid vesicles were always prepared from dry lipid films by dispersion in 2 mM Hepes, 1 mM EDTA (pH 7.4) buffer solution at a final concentration of 10 mg/ml and allowed to stand at room temperature for 1 h before adding the protein. Basic protein was dissolved in the same buffer and added to the lipid vesicle suspension while mixing with a vortex mixer. The basic protein/lipid ratio was 1 : 85 mol/mol which, assuming uniform distribution, corresponds to a vesicle surface coverage of 32%. After overnight incubation at 4°C uncomplexed vesicles were removed by centrifugation and 0.1 ml of vesicle suspension was filled into the ESR sample capillaries (i.d. 1 mm) and pelleted in a bench top centrifuge. Lipid/protein ratio of the pellet and supernatant was determined by a modified Lowry assay [16] and phosphate determination [17].

ESR spectroscopy. ESR spectra were recorded with a Jeol X-band ESR spectrometer (JES-PE-1X, Japan) using 100 kHz modulation technique. Typical instrumental setting: microwave power, 8 mW; scan range, 10 mT; modulation amplitude, 0.16 mT (G_{p-p}); gain, 10^3. The ±100 mV analog output of the spectrometer was digitized by a 12 ± 1 bit A/D converter and stored as 1 kiloword datafiles in a PDP 11/40 computer (Central Research Institute of Physics, Budapest) using softwares written by Dr. J. Czégé (this Institute). Spectra recorded at low label/lipid ratios were smoothed according to a polynomial algorithm; baseline drifts were corrected by adjusting vanishing first integrals. In most of the ESR spectra of lipid/protein complexes weak 'aqueous peaks' were observed due to the partitioning of 16-SASL between the membrane and aqueous phases; the integrated intensity of this spectrum component was < 5% for DMPC-MBP and < 1% for DMPG-MBP complexes. These overlapping aqueous peaks were digitally subtracted using our ESR software package written in Fortran.

Theoretical line shape analyses. The translational diffusion of lipids was measured from the spectral effects of spin–spin interaction. At low label/lipid ratios (0.1–2 mol%) the observed linewidth can be written as,

$$T_{2,\mathrm{obs}}^{-1} = T_2^{-1} + T_{2,\mathrm{HH}}^{-1} + T_{2,\mathrm{NN}}^{-1} \qquad \text{label/lipid} < 2\ \text{mol\%} \tag{1}$$

where T_2^{-1} is the intrinsic linewidth, $T_{2,\mathrm{HH}}^{-1}$ and $T_{2,\mathrm{NN}}^{-1}$ are due to exchange effects of the unresolved proton and nitrogen hyperfine structures. The line broadening terms $T_{2,\mathrm{HH}}^{-1}$ and $T_{2,\mathrm{NN}}^{-1}$ can be separated by the method of Bales [18]. Sachse et al. [19] explored several methods for the measurement of the translational diffusion based on different terms in Eqn. 1; molecular collision rates were determined from exchange narrowing of the unresolved proton hyperfine structure and from exchange/dipole broadening of the nitrogen hyperfine structure. The two contributions to $T_{2,\mathrm{NN}}^{-1}$, namely spin exchange and dipole–dipole interaction, were separated by their different temperature dependencies. In the range of intermediate label/lipid ratios (2–8 mol%) the contribution to line width of the exchange averaged proton hyperfine structure can be neglected [19] and the dominant term in Eqn. 1 is $T_{2,\mathrm{NN}}^{-1}$. The spectral effects of its two contributions can be separated more readily as the nitrogen hyperfine structure begins to merge into a broad singlet due to spin exchange. Sackmann and Trauble [20] derived a line shape formula from the steady-state exchange-coupled Bloch equations,

$$\left(T_{2,\mathrm{eff}}^{-1} + 3\nu_{\mathrm{ex}}\right) u_{\mathrm{m}} - \nu_{\mathrm{ex}} \Sigma u_{\mathrm{m}'} + \left(\omega_{\mathrm{m}} - \omega\right) v_{\mathrm{m}} = 0 \tag{2}$$

$$\left(T_{2,\mathrm{eff}}^{-1} + 3\nu_{\mathrm{ex}}\right) v_{\mathrm{m}} - \nu_{\mathrm{ex}} \Sigma v_{\mathrm{m}'} + \left(\omega_{\mathrm{m}} - \omega\right) u_{\mathrm{m}} = -\gamma H_1 M_{\mathrm{m}} \tag{3}$$

where the subscripts m and m′ refer to the nitrogen nuclear quantum number ($m_1 = +1, 0, -1$), u and v are the x and y components of the transverse magnetization, $T_{2,\mathrm{eff}}^{-1}$ is the effective spin-spin relaxation time, and ν_{ex} is the exchange frequency. (Further notations: ω is the angular resonance frequency, γ is the giromagnetic ratio, H_1 is the microwave magnetic field, and M_{m} is the value of the steady-state magnetization in the direction of the applied magnetic field.) It should

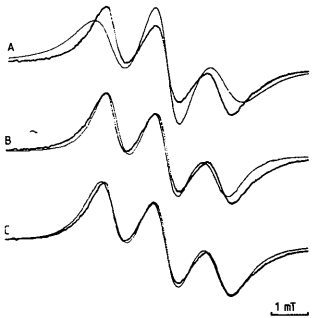

Fig. 1. Experimental ESR spectra of 16-SASL in dimyristoylphosphatidylcholine (DMPC) lipid vesicles and simulated line shapes based on the modified Bloch equations (Eqns. 2 and 3). The experimental spectrum (dotted line) is shown together with simulated line shapes (full line) assuming different combinations of spin exchange and dipole-dipole contributions. (A) Pure dipole-dipole broadening with no spin exchange contribution. (B) Exchange narrowing with no dipole-dipole contribution. (C) Best-fitting combination of spin exchange and dipole-dipole contribution. Experimental spectrum was recorded at 36 °C; total scan width = 10 mT.

be noted that no explicit reference is made to dipole–dipole interaction in Eqns. 2 and 3; its line broadening effect is absorbed in $T_{2,\mathrm{eff}}^{-1}$

$$T_{2,\mathrm{eff}}^{-1} = T_2^{-1} + T_{2,\mathrm{dd}}^{-1} \tag{4}$$

The imaginary part of the magnetization, $v = \Sigma\, v_m$, is proportional to the intensity of the ESR absorption.

Best-fitting simulated line shapes were adjusted by least-squares optimization; the parameter σ defined as

$$\sigma = \Sigma(Y_{\mathrm{exp}} - Y_{\mathrm{sim}})^2 / \Sigma Y_{\mathrm{exp}}^2 \tag{5}$$

was minimized by fitting T_2^{-1} to line shapes recorded at low label/lipid ratio and then varying $T_{2,\mathrm{dd}}^{-1}$ and ν_{ex}. (Y_{exp} are Y_{sim} are the ith point of the experimental and simulated spectra.) As illustrated in Fig. 1 reasonable fits could be obtained only if a combination of dipolar and spin exchange contributions were assumed. At high spin label mole fractions ($c > 0.02$) least-squares optimization always gave a unique combination for the relative contributions of ν_{ex} and $T_{2,\mathrm{dd}}^{-1}$ to the observed line broadening and line shape changes for which the parameter σ was minimal.

Results

Pure lipid vesicles

ESR spectra of 16-SASL in dimyristoylphosphatidylglycerol (DMPG) bilayers using various label/lipid mole fractions are shown in Fig. 2. These spectra were recorded at 36 °C in the liquid crystalline phase of DMPG and so motionally averaged three-line spectra were observed. On increasing the label/lipid mole fraction a Lorentzian line broadening was first detected (spectra A and B in Fig. 2) and then the spectral effects of spin exchange were dominating as expected for intermediate label/lipid mole fractions (spectra C and D in Fig. 2). Essentially similar results were obtained for dimyristoylphosphatidylcholine (DMPC) vesicles (data not shown). The experimental spectra are shown together with best-fitting simulated spectra in order to illustrate the quality of the simulations. Best-fitting simulations for intermediate label/lipid mole fractions were obtained with significantly greater contributions from the spin exchange (ν_{ex}) than the dipole-dipole ($T_{2,\mathrm{dd}}^{-1}$) terms to the line broadening as the nitrogen hyperfine structure began to collapse into an exchange averaged line shape. Monomolecular lateral diffusion coefficients calculated from these simulations and simulation parameters are summarized in Table I.

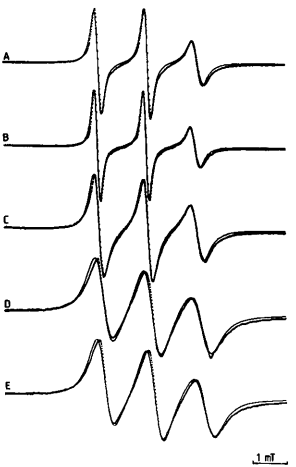

Fig. 2. Experimental ESR spectra of 16-SASL (thick dotted lines) in dimyristoylphosphatidylglycerol (DMPG) bilayers using various spin label concentrations and best-fitting simulated line shapes based on Eqns. 2 and 3 (full lines). All experimental spectra were recorded at 36 °C. Label/lipid mole fraction: (A) 0.010, (B) 0.020, (C) 0.038, (D) 0.070, and (E) 0.106. Simulation parameters of the best-fitting theoretical spectra are summarized in Table I.

TABLE I

Best-fitting simulation parameters and monomolecular lateral diffusion coefficients D_T of 16-SASL spin label in dimyristoylphosphatidylcholine (DMPC) and dimyristoylphosphatidylglycerol (DMPG) bilayers in the absence and presence of myelin basic protein (MBP)

All spectral data were calculated from fluid phase spectra recorded at 36°C.

	Label/lipid mol fraction, c	Intrinsic linewidth, T_2^{-1} (MHz)	Dipole broadening, $T_{2,dd}^{-1}$ (MHz)	Spin exchange frequency, ν_{ex} (MHz)	$10^7 D_T$ ($cm^2 \cdot s^{-1}$)
Pure DMPC vesicles	0.010	2.4	0.0	1.1	
	0.020	2.4	0.0	2.4	
	0.038	2.4	0.1	3.9	
	0.074	2.4	1.5	7.0	
	0.107	2.4	1.7	11.3	
	0.137	2.4	2.3	14.4	1.63
DMPC-MBP complex	0.010	1.7	0.0	1.6	
	0.020	1.7	0.0	2.4	
	0.038	1.7	1.1	3.9	
	0.061	1.7	1.4	6.5	
	0.097	1.7	1.5	11.2	
	0.123	1.7	1.7	13.9	1.78
Pure DMPG vesicles	0.010	2.4	0.0	1.3	
	0.020	2.4	0.0	2.0	
	0.038	2.4	1.5	3.7	
	0.070	2.4	1.9	8.7	
	0.106	2.4	2.2	8.6	
	0.136	2.4	3.0	9.2	1.18
DMPG-MBP complex	0.010	2.8	0.0	1.5	
	0.020	2.8	0.6	1.7	
	0.038	2.8	2.1	1.6	
	0.074	2.8	2.5	2.6	
	0.138	2.8	3.2	4.2	< 0.41

Lipid-protein complexes

Upon adding basic protein to preformed DMPC vesicles no apparent spectral changes were observed; comparing the best-fitting simulated spectra (dotted lines in Fig. 3) with those fitted to the spectra of pure DMPC vesicles no significant differences could be established (Table I). An entirely new pattern was recorded after the addition of basic protein to DMPG vesicles. The qualitative differences discussed below are rather striking even from a superficial comparison of the two spectrum series shown in Figs. 2 and 4. Here again the simulated spectra are overlaid with the experimental spectra in order to illustrate that the quality of these simulations is not inferior to those of pure lipid spectra. Best-fitting spectral parameters, including the intrinsic linewidths and the line broadenings due to dipole–dipole interaction and spin exchange are summarized in Table I. As expected from the line shape changes the dipole-dipole line broadening ($T_{2,dd}^{-1}$ term) became comparable to the linewidth effects of spin exchange (ν_{ex} term) for intermediate label/lipid mole fractions.

When using C-5 or C-14 positional isomers a motionally restricted spectral component could also be resolved both in DMPC-MBP and DMPG-MBP complexes ([10] and T. Páli and L.I. Horváth, unpublished results). It should be noted that this second component is more difficult to resolve with 16-SASL used in this work because its spectrum is dominated by the very narrow fluid component ($f_{im} < 0.15$) and hence in all subsequent line shape analyses the motionally restricted component was neglected.

Lateral diffusion coefficients

The spin exchange frequency ν_{ex} is proportional to the collision frequency ν_{coll} [21],

$$\nu_{ex} = 2I/(2I+1) \cdot p_{ex} \cdot \nu_{coll} \tag{6}$$

where I is the ^{14}N nuclear spin quantum number and p_{ex} is the probability of spin exchange on collision. In the case of lipid membranes $p_{ex} = 1/2$ in good approximation assuming collision pair lifetimes of $> 2 \cdot 10^{-11}$ s [22]. The diffusion process can be described by the hopping motion of lipid molecules in a two-dimensional hexagonal lattice. The lateral diffusion coefficient D_T is then given by

$$D_T = \frac{\lambda^2}{24} \frac{\nu_{coll}}{c} \tag{7}$$

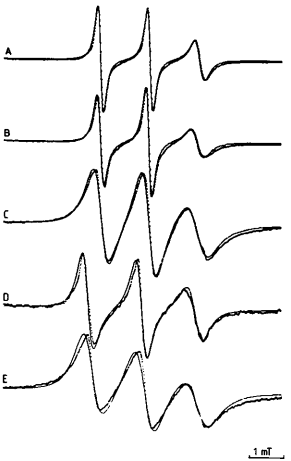

Fig. 3. Difference ESR spectra of 16-SASL (thick dotted lines) in dimyristoylphosphatidylcholine bilayers in the presence of protein (DMPC/MBP, ratio 1:85) using various spin label concentrations after subtracting the aqueous component. All experimental spectra were recorded at 36 °C. Best fitting simulated line shapes based on Eqns. 2 and 3 are overlaid with the experimental spectra (full lines). Label/lipid mole fraction: (A) 0.010, (B) 0.020, (C) 0.038, (D) 0.061, and (E) 0.097. Simulation parameters of the best-fitting theoretical spectra are summarized in Table I.

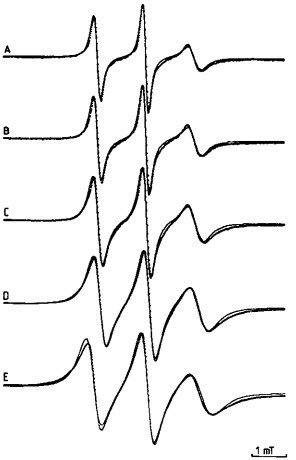

Fig. 4. Difference ESR spectra of 16-SASL (thick dotted lines) in dimyristoylphosphatidylglycerol bilayers in the presence of protein (DMPG/MBP, ratio 1:85) using various concentrations of the spin label. Aqueous components were subtracted by using 16-SASL in water reference spectra. All experimental spectra were recorded at 36 °C. Best fitting simulated line shapes based on Eqns. 2 and 3 are overlaid with the experimental spectra (full lines). Label/lipid mole fraction: (A) 0.010, (B) 0.020, (C) 0.038, (D) 0.074, and (E) 0.138. Simulation parameters of the best-fitting theoretical spectra are summarized in Table I.

where λ is the lattice spacing and c is the mole fraction. Since the collision frequency linearly depends on the mole fraction of spin label the lateral diffusion coefficient D_T can be determined from the gradient of $\nu_{coll} = \nu_{coll}(c)$ curves.

The concentration dependence of the collision frequency for pure DMPC and DMPG vesicles and lipid-protein complexes prepared with these two phospholipids is shown in Fig. 5. As expected the experimental points could be fitted well with straight lines in every case; typical correlation coefficients (r^2) of linear regression were at least 0.97. The lateral diffusion coefficients D_T calculated from the gradients of concentration dependence assuming a typical lattice spacing of 0.8 nm [23] were $1.6 \cdot 10^{-7}$ and $1.7 \cdot 10^{-7}$ cm$^2 \cdot$ s^{-1} for DMPC vesicles and DMPC-MBP complexes, respectively, whereas a somewhat lower lateral diffusion coefficient of $1.2 \cdot 10^{-7}$ cm$^2 \cdot$ s^{-1} was measured for DMPG vesicles and a significantly lower value of $4.1 \cdot 10^{-8}$ cm$^2 \cdot$ s^{-1} for DMPG-MBP complexes (Table I). It should

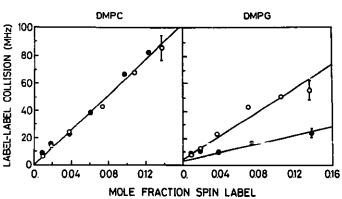

Fig. 5. Bimolecular label-label collision frequency ν_{coll} obtained from best-fitting simulated spectra as a function of mole fraction σ 16-SASL in dimyristoylphosphatidylcholine (DMPC) and dimyristoylphosphatidylglycerol (DMPG) bilayers in the absence (open symbols) and presence (full symbols) of basic protein. Error bars indicate a collision frequency range over which the parameter σ defined in Eqn. 4 increased by 5%.

be noted that the same evaluation for DMPG-MBP complexes was less reliable because all the experimental data points were very low throughout the mole fraction range used in this study and were probably close to the sensitivity limit of the method. Clearly, at slow rates of spin exchange the two contributions $T_{2,dd}^{-1}$ and ν_{ex} to the linewidth (see Eqns. 2–4) are more difficult to separate unambiguously and hence the lateral diffusion coefficient of $4.1 \cdot 10^{-8}$ cm$^2 \cdot$ s^{-1} should be regarded as an upper limit in this case.

Discussion

Membrane spectroscopy provides a very detailed insight into various molecular motions of proteins and lipids. Clearly, the motional coupling of lipids and proteins must play an important role in interfacing the membrane components and sealing the membrane. Spin label ESR has a rather suitable timescale for mapping the gradient in molecular dynamics at the interface of membrane proteins. A less studied aspect of this motional coupling is the modulation of lipid lateral diffusion by proteins. A theoretical estimate for the lateral diffusion of protein and lipid molecules has been given by Saffmann and Delbrück [24] (for a review, see Ref. 25). Since the lateral diffusion of membrane proteins is governed by the viscous drag at the interface and is influenced by the molecular size to lesser extent, D_T typically varies in the range of $5 \cdot 10^{-9}$–$5 \cdot 10^{-8}$ cm$^2 \cdot$ s^{-1} for proteins with hydrodynamic radii of 0.3–3.0 nm [24]. The lateral diffusion of lipids is inherently faster according to fluorescent recovery after photobleaching (FRAP) experiments: $5 \cdot 10^{-8}$–$2 \cdot 10^{-7}$cm$^2 \cdot$ s^{-1} [24–25]. Spin label ESR is also suitable for measuring lipid lateral diffusion using 16-SASL in conjunction with the Heisenberg spin exchange method [1]. Such measurements give greater diffusion coefficients than those obtained from FRAP [25] and ESR imaging experiments [26] since the range of motion detected by the Heisenberg spin exchange method is less than 1.2 nm and the lifting off motions associated with rotational isomerism can separate nearest neighbour labelled acyl chains beyond their magnetic radii thereby resulting in more molecular encounters.

The major result of the present spin label ESR experiments is that the lateral diffusion of various phospholipids is modulated rather selectively by basic protein. The diffusion coefficient of the spin probe in DMPC-MBP complexes remained unchanged as compared to the value observed in pure DMPC vesicles, whereas that in DMPG-MBP complexes was significantly less than in pure DMPG vesicles and was close to the sensitivity limit of the Heisenberg spin exchange method (Figs. 3 and 4, and Table I). The lateral diffusion coefficient in DMPC-MBP complexes ($1.7 \cdot 10^{-7}$ cm$^2 \cdot$ s^{-1}) lies in the range observed for fluid lipid bilayers by spin label ESR experiments [19,25] and suggests no interaction between basic protein and DMPC in agreement with earlier results (for a review, see Ref. 11). The diffusion coefficient in DMPG-MBP complexes, on the other hand, was $4.1 \cdot 10^{-8}$ cm$^2 \cdot$ s^{-1} indicating a restricted lateral diffusion as a consequence of lipid–protein interaction. A possible explanation of the slow lateral diffusion is that certain lipids, which interact with the basic protein with great selectivity and form short-living segregated domains, undergo slow co-diffusion with the protein.

Selective association of acidic lipids with membrane proteins can be explained by electrostatic and hydrophobic interactions [2,3,11,25]. From a comparison of the effects of basic protein and polylysine the relative contributions of hydrophobic and electrostatic interactions could be estimated [27]. Labeling experiments with a hydrophobic photolabel also suggested that the basic protein can penetrate into bilayers of acidic lipids deeper than the polar headgroup region [28]. Therefore it seems that basic protein, as it interacts with the membrane surface, exposes a hydrophobic surface for contact lipid–protein interaction in the interfacial region. This is consistent with the shorter T_1 values obtained in ^{2}H-NMR experiments which also indicate a slowing down of acyl chain motions [29,30].

The free diffusion of lipids off the protein can be restricted in the interfacial region where the charged lipid headgroups are in contact with positively charged amino acids of the protein. The off-rates of DMPC and other zwitterionic lipids has proved to be diffusion controlled and virtually unaffected by integral membrane proteins, whereas the off-rates of acidic lipids such as DMPG are less by a factor of 1.5–3 at the interface of proteins depending on their relative association constants [31–33]. Applying the same model [3,34] to the case of basic protein an unchanged one-to-one lipid exchange and diffusion controlled lateral movement is expected for the zwitterionic DMPC and a slowing down by 30–50% for DMPG because of its specificity. Since the observed spectra indicate a greater change in the collision frequency (Table I) we conclude that the restricted lateral diffusion in DMPG/MBP complexes is partly due to the slowing down of one-to-one lipid exchange and partly due to lipid-protein co-diffusion. An unambiguous determination of these two factors requires macroscopic (imaging or FRAP) methods in conjunction with the Heisenberg spin exchange method.

Acknowledgments

We gratefully thank Dr. D. Marsh (Göttingen, F.R.G.) for providing phosphatidylglycerol and Dr. G.J. Tigyi (this Institute) for purifying basic protein. This

project was supported by the Hungarian Academy of Sciences (OTKA 175/1988 to L.I.H.).

References

1 Marsh, D. (1988) in Physical Properties of Biological Membranes and Their Functional Implications (Hidalgo, C., ed.), Chapter 4, pp. 123–145, Plenum Press, New York.
2 Devaux, P.F. and Seigneuret, M. (1985) Biochim. Biophys. Acta 822, 63–125.
3 Marsh, D. (1985) in Progress in Protein-Lipid Interactions (Watts, A. and De Pont, J.J.H.M., eds.), pp. 143–172, Elsevier Science Publishers, Amsterdam.
4 Marsh, D. (1986) in Supramolecular Structure and Function (Pifat-Mrzljak, G., ed.), pp. 48–62, Springer-Verlag, Berlin-Heidelberg.
5 Boggs, J.M. and Moscarello, M.A. (1978) J. Membr. Biol. 39, 75–96.
6 Görissen, H. and Marsh, D. (1986) Biochemistry 25, 2904–2910.
7 De Kruijff, B., Rietveld, A., Jordi, W. Berkhout, T.A., Demel, R.A., Görissen, H. and Marsh, D. (1988) in NATO ASI Series H16, (Op den Kamp, J.A.F., ed.), pp. 257–269, Springer-Verlag, Berlin-Heidelberg.
8 Jancsik, V. and Horváth, L.I. (1985) Biochim. Biophys. Acta 820, 283–288.
9 Kim, J. and Kim, H. (1986) Biochemistry 25, 7867–7874.
10 Sankaram, M.B., Brophy, P.J. and Marsh, D. (1986) in PRoceedings of 12th International Conference on Magnetic Resonance in Biological Systems, Todtmoos, Germany, p. 141.
11 Boggs, J.M., Moscarello, M.A. and Papahadjapoulos, D. (1982) in Lipid-Protein Interactions (Jost, P.C. and Griffith, O.H., eds.), Vol. 2, pp. 1–51, Academic Press, New York.
12 Surewicz, W.K., Moscarello, M.A. and Mantsch, H.H. (1987) Biochemistry 26, 3881–3886.
13 Smith, R. (1977) Biochim. Biophys. Acta 470, 170–184.
14 Páli, T., Ebert, B. and Horváth, L.I. (1987) Biochim. Biophys. Acta 904, 346–352.
15 Tigyi, G.J., Balázs, L., Monostori, É. and Andó, I. (1984) Mol. Immunol. 21, 889–894.
16 Lowry, O.H., Rosebrough, N.J., Farr, A.L. and Randall, R.J. (1951) J. Biol. Chem. 193, 265–275.
17 Eibl, H. and Lands, W.E.M. (1969) Anal. Biochem. 30, 51–51.
18 Bales, B.L. (1982) J. Magn. Reson. 48, 418–430.
19 Sachse, J.-H., King, M.D. and Marsh, D. (1987) J. Magn. Reson. 71, 385–404.
20 Sackmann, E. and Trauble, H. (1972) J. Am. Chem. Soc. 94, 4482–4510.
21 Devaux, P.F., Scandella, C.J. and McConnell, H.M. (1973) J. Magn. Res. 9, 474–485.
22 Plachy, W.Z. and Kivelson, D. (1967) J. Chem. Phys. 47, 3312–3318.
23 Watts, A., Marsh, D. and Knowles, P.S. (1978) Biochemistry 17, 1792–1801.
24 Saffmann, P.G. and Delbrück, M. (1975) Proc. Natl. Acad. Sci. USA 72, 3111–3113.
25 Clegg, R.M. and Vaz, W.L.C. (1985) in Progress in Protein-Lipid Interactions (Watts, A. and De Pont, J.J.H.H.M., eds.), Vol. 1, pp. 173–229, Elsevier, Amsterdam.
26 Hornak, J.P., Moscicki, J.K., Schneider, D.J. and Freed, J.H. (1986) J. Chem. Phys. 84, 3387–3395.
27 Boggs, J.M., Wood, D.D. and Moscarello, M.A. (1981) Biochemistry 20, 1065–1073.
28 Boggs, J.M., Rangaraj, G. and Koshy, K.M. (1988) Biochim. Biophys. Acta 937, 1–9.
29 Sixl, F., Brophy, P.J. and Watts, A. (1984) Biochemistry 23, 2032–2039.
30 Bloom, M. and Smith, I.C.P. (1985) in Progress in Protein-Lipid Interactions (Watts, A. and De Pont, J.J.H.H.M., eds.), Vol. 1, pp. 61–88, Elsevier, Amsterdam.
31 Ryba, N., Horváth, L.I., Watts, A. and Marsh, D. (1987) Biochemistry 26, 3234–3240.
32 Horváth, L.I., Brophy, P.J. and Marsh, D. (1988) Biochemistry 27, 46–52.
33 Horváth, L.I., Brophy, P.J. and Marsh, D. (1988) Biochemistry 27, 5296–5304.
34 Marsh, D. and Horváth, L.I. (1989) in Advanced EPR in Biology and Biochemistry (Hoff, A.J., ed.), Elsevier, in press.